The Nepali Mathematical Sciences Report, Vol. 37, No. 1& 2 2020: 71-79
DOI:https://doi.org/10.3126/nmsr.v37i1-2.34093

RHEOLOGICAL PARAMETER ANALYSIS IN GENERALIZED BULK MIXTURE MASS FLOW MODEL

PUSKAR R. POKHREL[1], PARAMESHWARI KATTEL[2], KHIM B. KHATTRI[3] AND JEEVAN KAFLE[4]

[1]*Department of Mathematics, Ratna Rajya Laxmi Campus, Tribhuvan University, Nepal*
[2]*Department of Mathematics, Tri-Chandra Multiple Campus, Tribhuvan University, Nepal*
[3]*Department of Mathematics, School of Science, Kathmandu University, Nepal*
[4]*Central Department of Mathematics, Tribhuvan University, Kathmandu, Nepal*

Correspondence to: Parameshwari Kattel, Email: pkattel526@gmail.com

Abstract: Pokhrel et al. [33] recently developed a generalized quasi two-phase bulk mixture model for mass flow. This model has been constructed by employing full dimensional two-phase mass flow model equations. The model is a set of coupled partial differential equations which is characterized by some new mechanical and dynamical aspects of generalized bulk and shear viscosities, pressure, velocities and effective friction for the mixture where all these are evolving as functions of several dynamical variables, physical parameters, inertial and dynamical coefficients and drift factors. They formulated pressure and rate-dependent Coulumb-viscoplastic rheology of the mixture mass flow to describe the model equation. Rheological behavior of the flow dynamics affects the whole dynamics of mixture mass flow. So, in this paper, the relations of mixture pressure and viscosity with respect to pressure drifts and solid volume fractions are studied to describe the rheological behavior of the generalized bulk mixture mass flow model. Moreover, the behaviour of mixture viscosities with respect to isotrophic drifts are also analyzed. We also present the simulation result for the time evolution of the drift induced full dynamical mixture pressure of the material exited from a silo gate that moves downslope along a channel.

Keywords: Rheological parameter analysis; Mixture mass flow model; Velocities and pressures; Mixture densities; Velocity and pressure drifts.
AMS (MOS) Subject Classification. 74A-10, 76A-99.

1. Introduction

Mass flow and mass wasting phenomena are common processes in industrial and geophysical contexts [17]. Debris flow as a typical example of geophysical mass flow, is effectively a mixture flow, which contains solid particles and viscous fluid. During these events, the mixture material undergoes rapid motion and large shearing [18, 19, 38]. These features together with the evolving mixture density provides debris flow with potentially huge energy and destructive power [18, 19]. Pudasaini [38] made significant advancement in the modeling and simulation of two phase debris flow by incorporating important aspects of two-phase debris

Received: May 23, 2020 Accepted/Published Online:January, 2021.

flow, such as virtual mass force, non-Newtonian viscous stress and generalized drag. Employing this model and the simulation techniques, there are significant studies of debris flow dynamics and obstacle-interactions both in subaerial and submarine environments [11, 12, 13, 14, 15, 16, 17, 18, 19, 20, 21, 22, 32, 39, 40]. This model is also used to develop quasi two-phase bulk mixture models, some parameter analyses and simulations [23, 24, 25, 26, 27, 34, 35]. Pokhrel [32] and Pokhrel and Tuladhar [36] described the debris flow behavior by developing more generalized eigenvalues of two phase mass flow model.

The mixture motion and the settlement of geophysical mass are described by constitutive law, which is modelled by the viscoplastic rheology [1, 2, 5, 10]. Iverson [7], Iverson and Denlinger [9], Pudasaini et al. [37], and Massoudi [28, 29] used the total stress in a mixture as the sum of solid and fluid-phases stress tensors. Domnik et al. [4] developed the pressure and rate-dependent Coulomb viscoplastic rheological model to describe the full dynamics of the rapid flows of granular materials down the channels impinging on rigid walls. Pokhrel et al. [33] made it possible to extend the pressure- and rate-dependent Coulomb-viscoplastic granular flow rheology to the flow of debris mixtures. Pokhrel et al. [33] constructed the mixture stress tensor by employing the mixture pressure, velocity, mixture shear viscosity and mixture strain-rate tensor.

Nepal has diversified topography from the world's tallest mountain to the low flat Terai plains. Due to the young mountain geology of the seismically active region and significant precipitation, Nepal is time and often hit by catastrophic avalanches, landslides, debris flows and mud flows. Most often, such flows exhibit a true mixture flow behaviour of the solid and fluid phases and reveal strong interactions between them. Moreover, industrial mass flows including pharmaceuticals and food processes include granular to multiphase mixture mass flows. In most of the these cases, the mixture mass is exited form silo gate, flown down for processing and ends with packing. Generalized quasi two-phase mixture mass flow model developed by Pokhrel et al. [33] and simulations therein describe the reconstruction of the two-phase mass mass flow dynamics. It is computationally faster than the two-phase flow, where as it is more accurate than the existing single phase models. The depth resolved model equations are also useful to describe the vertical profile of velocity and particle concentration. So the model is more useful than the depth-integrated model in the predictions of the dynamics and impact forces/pressures in case of abruptly changing topography, especially when the flow encounters obstacles [24]. For the correct and reliable description of the debris flow behavior, we need more accurate description of mixture pressures and viscosity. Here, we focus on the rheological part of the model developed in Pokhrel et al. [33] and study some parameter behaviours.

2. The Flow Rheological Model

First, we present the generalized quasi two-phase bulk mixture model for mass flow [33] out of which the rheological equations and the expression for the drift induced barycentric pressure have been employed in our study. Let u_m and w_m be the components of velocities for the mixture flow in the downslope (x-) and the perpendicular to the flow (z-) directions, as in Fig. 1, respectively. The suffix m stands for the mixture, and p_m denotes the mixture pressure [33] are as follows:

$$\frac{\partial u_m}{\partial x} + \frac{\partial w_m}{\partial z} = 0, \tag{2.1}$$

$$\begin{aligned}\frac{\partial u_m}{\partial t} + \frac{\partial}{\partial x}(\Lambda_{uu} u_m^2) + \frac{\partial}{\partial z}(\Lambda_{uw} u_m w_m) = f_x - \frac{\partial p_m}{\partial x} \\ + 2\frac{\partial}{\partial x}\left[\Lambda_{\eta_u}\frac{\partial(\Lambda_u u_m)}{\partial x}\right] + \frac{\partial}{\partial z}\left[\Lambda_{\eta_u}\frac{\partial(\Lambda_u u_m)}{\partial z} + \Lambda_{\eta_w}\frac{\partial(\Lambda_w w_m)}{\partial x}\right],\end{aligned} \tag{2.2}$$

$$\begin{aligned}\frac{\partial w_m}{\partial t} + \frac{\partial}{\partial x}(\Lambda_{uw} u_m w_m) + \frac{\partial}{\partial z}(\Lambda_{ww}\, w_m^2) = f_z - \frac{\partial p_m}{\partial z} \\ + \frac{\partial}{\partial x}\left[\Lambda_{\eta_u}\frac{\partial(\Lambda_u u_m)}{\partial z} + \Lambda_{\eta_w}\frac{\partial(\Lambda_w w_m)}{\partial x}\right] + 2\frac{\partial}{\partial z}\left[\Lambda_{\eta_w}\frac{\partial(\Lambda_w w_m)}{\partial z}\right].\end{aligned} \tag{2.3}$$

In the equations (2.1)-(2.3), t is time, $u_m = (\alpha_s + \lambda_u\alpha_f)u_s$, $w_m = (\alpha_s + \lambda_w\alpha_f)w_s$, $p_m = (\alpha_s + \lambda_p\alpha_f)p_s$, where λ_u, λ_w are velocity drift factors, and λ_p is pressure drift factor. α_s, $\alpha_f(= 1 - \alpha_s)$ respectively denote the volume fractions for the solid and fluid components in the mixture, The suffices s and f stand for the solid and fluid phases, respectively. p_s and p_f are the solid and fluid phase pressures in the mixture flow. $\mathbf{f} = (f_x, f_z)$, where f_x and f_z are the components of the gravitational acceleration, $\Lambda_{\eta_u} = \nu_s^e\alpha_s + \lambda_u\nu_f\alpha_f$, $\Lambda_{\eta_w} = \nu_s^e\alpha_s + \lambda_w\nu_f\alpha_f$ are the mixture viscosities, where ν_s^e is the effective kinematic viscosity for the solid, and ν_f is the kinematic viscosity for the fluid. The model constitutes a set of coupled partial differential equations for mass ((2.1)) and momentum ((2.2) and (2.3)) balances. The model is characterized by some mechanical and dynamical aspects of generalized bulk and shear viscosities, pressure, velocities and effective friction for the mixture where all these are evolving as functions of several dynamical variables, physical parameters, inertial and dynamical coefficients and drift factors. The flow rheology is intrinsic to this model and includes the physical and dynamical properties of both the solid and fluid components [33]. In the model, the Cauchy stress tensor for the mixture is:

$$\boldsymbol{\sigma}_m = -p_m\mathbf{I} + 2\Lambda_{\eta_m}\mathbf{D}_m, \tag{2.4}$$

where, p_m is the normalized pressure

$$p_m = \frac{(\alpha_s + \lambda_p\alpha_f)\ (\alpha_s\rho_s p_s + \alpha_f\rho_f p_f)}{\alpha_s\rho_s + \lambda_p\alpha_f\rho_f}. \tag{2.5}$$

This is called the drift induced generalized barycentric pressure for the mixture flow, $p_f = \lambda_p p_s$, and the pressure drift λ_p has important role in the pressure dynamics. $\mathbf{I}$ is the identity square matrix, and Λ_{η_m} is the generalized mixture viscosity:

$$\Lambda_{\eta_m} = \frac{1}{2}\nu_s^e\alpha_s\ (\Lambda_u + \Lambda_w) + \frac{1}{2}\nu_f\alpha_f\ (\lambda_u\Lambda_u + \lambda_w\Lambda_w). \tag{2.6}$$

Here, $\mathbf{D}_m = \frac{1}{2}[\nabla\mathbf{u}_m^\Lambda + (\nabla\mathbf{u}_m^\Lambda)^T]$ is the strain-rate tensor for mixture, where $\mathbf{u}_m^\Lambda = (\Lambda_u u_m, \Lambda_w w_m)$, $\Lambda_u = 1/(\alpha_s + \lambda_u\alpha_f)$, $\Lambda_w = 1/(\alpha_s + \lambda_w\alpha_f)$, $u_f = \lambda_u u_s$, $w_f = \lambda_w w_s$, and T denotes the transpose operator. Bulk viscosity represented by (2.6) captures the mechanics of mixture rheology. Solid volume fraction α_s has the major influence in the model equations via inertial and dynamical coefficients, pressure parameters, velocity and pressure definition. Importantly, the rheology defines and controls the flow behavior and flow regimes

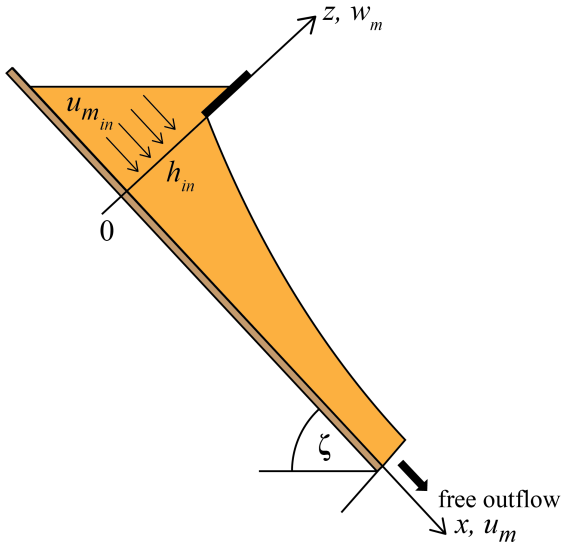

FIGURE 1. Side view of the rapid flow of debris material along an inclined chute. $u_{m_{in}}, h_{in}$ are initial velocities and heights of the mixture flow, ζ is the inclination angle [33].

of the mixture flow. The effective kinematic viscosity for solid is

$$\nu_s^e = \nu_s + \frac{\tau_{y_s}}{||\mathbf{D}_m||},$$

where ν_s^e is kinematic viscosity, τ_{y_s} is yield stress. The effective kinematic viscosity approaches to infinity as $||\mathbf{D}_m|| \to 0$. To control this problem in computation, Domnik et al. [4], von Boetticher et al.[41, 42] introduced the exponential factor m_y, and Pokhrel et al. [33] added the strain-rate tensor for mixture $\mathbf{D}_m$ as

$$\nu_s^e = \nu_s + \frac{\tau_{y_s}}{||\mathbf{D}_m||}\left(1 - e^{-m_y||\mathbf{D}_m||}\right).$$

Domnik et al. [4] demonstrated a pressure dependent yield stress for granular flow, and Pokhrel et al. [33] added a pressure dependent yield stress $\tau_{y_s} = \tau_c + \tau_p p_m/\Lambda_p$, where τ_c is cohesion, for mixture flow to capture the flow behavior of bulk mixture mass flow. This forms a Drucker-Prager yield criterion [31] as

$$\sqrt{\Pi_{\sigma_{D_m}}} \geqslant \tau_p p_m,$$

where $\Pi_{\sigma_{D_m}}$ is the second invariant of the deviatoric stress tensor [31]. If the x- and z-directional velocity drifts λ_u and λ_w are identical, i.e., $\lambda_u = \lambda_w$ (isotropic drifts). During the mass flow, the material behaves as a Newtonian fluid for $\tau_{y_s} = 0$ for which effective viscosity is equal to kinematic viscosity, i.e., $\nu_s^e = \nu_s$. Then,

$$\Lambda_{\eta_m} = \frac{\nu_s\alpha_s + \lambda_u\nu_f\alpha_f}{\alpha_s + \lambda_u\alpha_f}. \tag{2.7}$$

Equation (2.7) gives the mixture viscosity that includes the terms of fluid volume fraction, velocity drift factor, and kinematic viscosities for solid and fluid.

3. Numerical Method

In this paper, the simulation to show the variation of mixture pressure in the channel downslope and the normal directions (Fig. 5) is performed using the extended *Nast2D* method, which is an expanded computer code based on the finite volume method for the numerical integration of the model for complex mixture mass flow of incompressible non-Newtonian fluids and solid grains [3, 4, 6]. Computational domains are discretized by using staggered grid which prevents potential pressure oscillations. Possible instabilities are avoided by using a mixture of central difference and donor-cell discretization. The x- and z-axes of the spatial domain are discretized into the maximum number of cells of equal sizes, whose centres are reserved for the mixture pressures p_m. The horizontal component of the mixture velocities u_m are placed at the midpoints of the vertical cell edges, where as the vertical component of mixture velocities w_m are at the midpoints of the

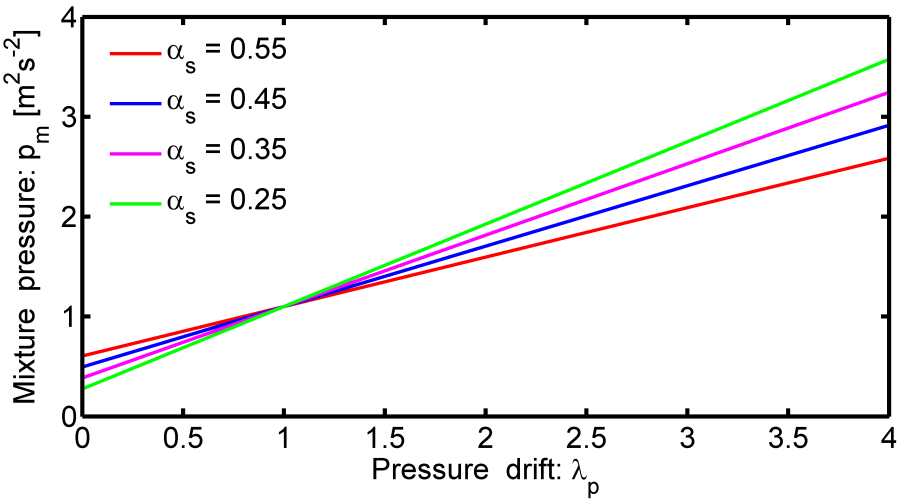

Figure 2. Variation of mixture pressure with pressure drift.

horizontal cell edges. The details of the full model discretization of the generalized quasi mixture models for mass flow [33] has been described in Khattri [25], and Khattri and Pudasaini [26].

4. Results and Discussion

Figure 2 reveals that the mixture pressure, as represented by the equation (2.5), varies linearly with the pressure drift. The chosen parameters are $\rho_f = 1100$ kg/m^3, $\rho_s = 2500$ kg/m ^{3}, $p_s = 1.1$ m^2/s^2 (as it is normalized by density), and four different values of α_s from 0 to 1 are chosen. For higher solid volume fraction (i.e., for denser flow), the mixture pressure is also higher until the pressure drift reaches to unity. On contrary, lower the solid volume fraction (i.e., for dilute flow), higher is the mixture pressure for $1 < \lambda_p \leq 4$. Result also shows that the mixture pressure increases along with the pressure drift. However, the rate of increment is higher for the lower value of α_s. Hence, for the given solid phase pressure, the mixture pressures with the increasing pressure drifts evolve differently for different particle concentrations in the mixture. Thus, beside the particle concentration, pressure drift also plays crucial role in the pressure drift induced mixture pressure dynamics. We note that when $\lambda_p = 1$, the pressure drift induced barycentric mixture pressure becomes the classical barycentric mixture pressure. In Fig. 2, all p_m coincide for $\lambda_p = 1$.

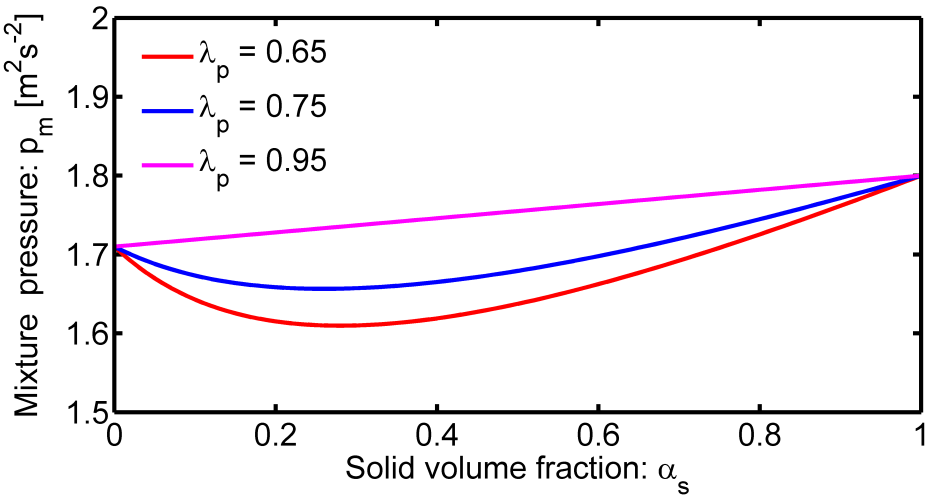

Figure 3. Variation of mixture pressure with solid volume fraction.

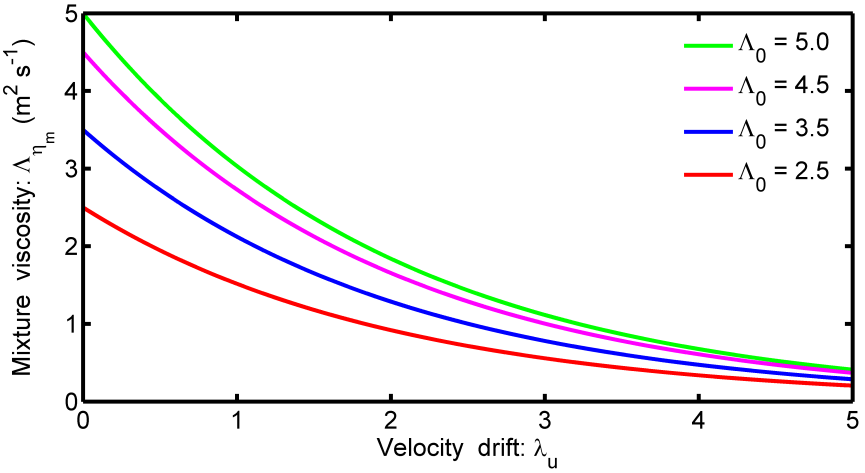

Figure 4. Variation of mixture viscosity with velocity drift.

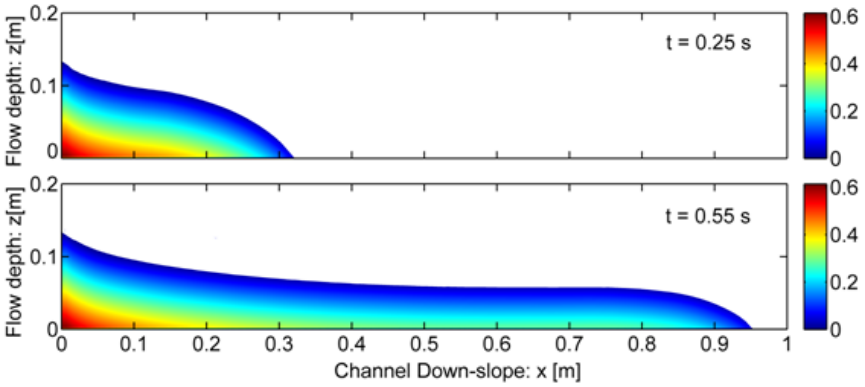

FIGURE 5. Time evolution of mixture pressure fields along the channel.

Figure 3 plots the drift induced barycentric mixture pressure p_m against the whole spectrum of the solid volume fraction $\alpha_s \in [0, 1]$ for three different values of the pressure drift $\lambda_p = 0.65, 0.75$ and 0.95. It shows that lower the pressure drift factor, more the mixture pressure drops non-linearly along the increasing solid volume fraction up to its certain value and again begin to increase beyond that value. However, in the phase limits ($\alpha_s \to 0$ and $\alpha_s \to 1$), the mixture pressures become identical irrespective of the values of the pressure drift.

Figure 4, as represented by the equation (2.7), shows that the mixture viscosity decreases exponentially with respect to isotropic velocity drift ($\lambda_u = \lambda_w \in [0, 5]$) for the different initial mixture viscosities $\Lambda_0 = 2.5$ m^2/s, $\Lambda_0 = 3.5$ m^2/s, $\Lambda_0 = 4.5$ m^2/s and $\Lambda_0 = 5.0$ m^2/s. In this case, we consider that the mixture is composed of 45% fluid and 55% solid. In Pokhrel et al. [33], the mixture velocity also drops exponentially with the increasing isotropic velocity drift λ_u for different values of α_s. Similarly in Khattri and Pudasaini [26], the mixture viscosity dropped non-linearly with the increasing strain-rate at a particular time for different values of α_s. In both of these cases, same initial mixture viscosity were considered. Here, we fixed the value of α_s and varied the initial mixture viscosities to obtain different non-linear behaviours.

To simulate the time evolution of the drift induced barycentric pressure during the flow of mixture material, we consider the initial set-up as given in Fig. 1. The mixture material with 55% solid and 45% fluid is released out of a silo gate and let it move along a channel with inclination $\zeta = 45^\circ$. The debris material enters into the channel at $x = 0$ m with an inlet height $h_{in} = 0.15$ m and an average inlet velocity of $u_{m_{in}} = 0.9$ m/s. Other chosen parameters are kinematic viscosity for solid $\nu_s = 0.3591$ m^2/s, and for fluid $\nu_f = 10^3$ m^2/s, Bingham exponent factor $m_y = 10$, pressure dependent yield stress parameter $\tau_p = \sin\phi = 0.5446$, cohesion $\tau_c = 60$ Pa (due to the bed friction angle $\delta = 25^\circ$, internal friction angle of the solid grains, $\phi = 33^\circ$). As in Khattri and Pudasaini [26], we have set the velocity and pressure drifts each close to unity, i.e., $\lambda_u, \lambda_w, \lambda_p \approx 1$.

Using aforementioned choices of initial set-up and parameters, Fig. 5 simulates the pressure fields along the channel for solid volume fraction $\alpha_s = 0.55$. The layered structures of the full dynamical mixture pressure along the channel originate both from the depth-dependence of the pressure (hydrostatic pressure contribution) and the flow dynamics (dynamical pressure contribution) as it moves down an inclined channel (with slope angle, $\zeta = 45^\circ$). Mixture pressure increases from the free surface to the channel bed due to the hydrostatic pressure contribution. Later on, the pressure decreases along the channel bed as the flow moves downslope along with the time elapses. It is because the gravitational acceleration causes a dilatational downslope motion. We further observe that the geometry of the pressure profile has some changes in the free surface as time elapses. But, the pressure is almost same around the channel bed since the mass is still flowing out of the silo gate even at $t = 0.55$ s [26].

5. Conclusions

Here, we focused on some rheological aspects of a generalized bulk mixture flow down a channel. The drift induced generalized mixture pressure against the pressure drift showed significant variations for different compositions of the mixture material. Mixture pressure revealed non-linear behaviour with increasing solid volume fractions for different pressure drifts. The mixture viscosity decreases with the increasing solid volume fraction for different initial mixture viscosities. The simulated mixture viscosity is rich in its physics and evolves mechanically as a coupled function of several physical and mechanical parameters. The mixture pressure along the channel decreases as it moves out of the silo gate. Moreover, it forms layered structure of increasing pressure from free surface to the channel bed. The estimation of mixture viscosity with velocity drifts is important to analyze the flow dynamics of mixture mass. Although the simulation presented here is in small scale, as future work, the modeling and computing techniques can be upscaled to industrial or even larger geophysical scales for the betterment of the processing in industries, and to estimate pressures and other field variables in hazard mitigation purpose and planing, especially in constructing the defense structures for hazard mitigation in disaster-prone mountains and coastal regions.

References

[1] C. Ancey, Plasticity and geophysical flows: A review, *J. Non-Newton. Fluid Mech.*, Vol. 142 (1–3), pp 4-35, 2007.

[2] N. J. Balmforth, I. Frigaard, Viscoplastic fluids: From theory to application, *J. Non-Newton. Fluid Mech.*, Vol. 142, pp 1-3, 2007.

[3] B. Domnik, S. P. Pudasaini, Full two-dimensional rapid chute flows of simple viscoplastic granular materials with a pressure-dependent dynamic slip-velocity and their numerical simulations, *J. Non-Newtonian Fluid Mech.*, Vol. 173, pp 72-86, 2012.

[4] B. Domnik, S.P. Pudasaini, R. Katzenbach, S. A. Miller, Coupling of full two-dimensional and depth-averaged models for granular flows, *J. Non-Newtonian Fluid Mechanics*, Vol. 201, pp 56-68, 2013.

[5] Y. Forterre, O. Pouliquen, Flows of dense granular media, *Annu. Rev. Fluid Mech.*, Vol. 40, pp 1-24, 2008.

[6] M. Griebel, T. Dornseifer, T. Neunhoeffer, *Numerical Simulation in Fluid Dynamics: A Practical Introduction*, Society for Industrial and Applied Mathematics, Philadelphia, 1997.

[7] R. M. Iverson, The physics of debris flows, *Rev. Geophys.*, Vol. 35(3), pp 245-296, 1997.

[8] R. M. Iverson, Elementary theory of bed-sediment entrainment by debris flows and avalanches, *J. Geophys. Res.*, Vol. 117(F03006), pp 197 - 200, 2012.

[9] R. M. Iverson, R. P. Denlinger, Flow of variably fluidized granular masses across three-dimensional terrain: 1. Coulomb mixture theory, *J. Geophys. Res.*, Vol. 106(B1), pp 537 -552, 2001.

[10] P. Jop, Y. Forterre, O. Pouliquen, A constitutive law for dense granular flows, Coulomb mixture theory, *Nature* Vol. 441 (7094), pp 727-730, 2006.

[11] J. Kafle, Dynamic Interaction Between a Two-phase Submarine Landslide and a Fluid Reservoir, MPhil Dissertation, School of Science, Kathmandu University, Nepal, 2014.

[12] J. Kafle, P. R. Pokhrel, K. B. Khattri, P. Kattel, B. M. Tuladhar, S. P. Pudasaini, Submarine landslide and particle transport in mountain lakes, reservoirs and hydraulic plants, *Annals of Glaciology*, Vol. 57(71), pp 232-244, 2016.

[13] J. Kafle, B. M. Tuladhar, Landslide-water interaction for partially submerged landslide, *Journal of Nepal Mathematical Society*, Vol. 1(1), pp 22-29, 2018.

[14] J. Kafle, Advanced Dynamic Simulations of Landslide Generated Tsunami, Submarine Mass Movement and Obstacle Interaction, PhD Dissertation, School of Science, Kathmandu University, Nepal, 2019.

[15] J. Kafle, P. Kattel, M. Mergili, J.-T. Fischer, S. P. Pudasaini, Dynamic response of submarine obstacles to two-phase landslide and tsunami impact on reservoirs, *Acta Mechanica*, Vol. 230(9), pp 3143-3169, 2019.

[16] J. Kafle, P. Kattel, Simulations for rotational symmetry through r.avaflow in the general two-phase mass flow model, *Journal of Nepal Mathematical Society*, Vol. 2(2), pp 45-60, 2019.

[17] P. Kattel, Dynamics of Quasi-Three-Dimensional and Two-Phase Mass Flows, MPhil Dissertation, School of Science, Kathmandu University, Nepal, 2014.

[18] P. Kattel, K. B. Khattri, P. R. Pokhrel, J. Kafle, B. M. Tuladhar, S.P. Pudasaini, Simulating glacial lake outburst floods with a two-phase mass flow model, *Annals of Glaciology*, Vol. 57(71), pp 349-358, 2016.

[19] P. Kattel, J. Kafle, J.-T. Fischer, M. Mergili, B. M Tuladhar, S. P. Pudasaini, Interaction of two-phase debris flow with obstacles, *Engineering Geology*, Vol. 242, pp 197-217, 2018.

[20] P. Kattel, B. M. Tuladhar, Interaction of two-phase debris flow with lateral converging shear walls, *Journal of Nepal Mathematical Society*, Vol. 1(2), pp 40-52, 2018.

[21] P. Kattel, Some Aspects of Multi-Phase Debris Flows: Dynamics, Flow-Obstacle-Interactions and Model Construction, PhD Dissertation, School of Science, Kathmandu University, Nepal, 2019.

[22] K. B. Khattri, Sub-diffusive and Sub-advective Viscous Fluid Flows in Debris and Porous Media, MPhil Dissertation, School of Science, Kathmandu University, Nepal, 2014.

[23] K. B. Khattri, S. P. Pudasaini, An Extended Quasi Two-Phase Mass Flow Model, *International Journal of Non-Linear Mechanics*, Vol. 106, pp 205-222, 2018.

[24] K. B. Khattri, J.-T. Fischer, M. Jaboyedoff, S. P. Pudasaini, Wet snow avalanche simulations to asses flow-obstacle-interactions and potential defense structure designs, Proceeding, International Snow Science Workshop, Innsbruck, Austria, pp 711-715, 2018.

[25] K. B. Khattri, Development, Discretization and Simulation of An Extended Quasi Two-Phase Mass Flow Model, PhD Dissertation, School of Science, Kathmandu University, Nepal, 2019.

[26] K. B. Khattri, S. P. Pudasaini, Channel flow simulations of a mixture with a full dimensional generalized quasi two-phase model, *Mathematics and Computers in Simulation*, Vol. 165, pp 280-305, 2019.

[27] K. B. Khattri, P. Kattel, B. M. Tuladhar, Some simulation results and parameter analyses of a generalized quasi two-phase bulk mixture model, *Journal of Nepal Mathematical Society*, Vol. 2(1), pp 45-56, 2019.

[28] M. Massoudi, Constitutive relations for the interaction force in multicomponent particulate flows, *Int. J. Non-Linear Mech.*, Vol. 38, pp 313-336, 2003.

[29] M. Massoudi, A mixture theory formulation for hydraulic or pneumatic transport of solid particles, *Int. J. Eng. Sci.*, Vol. 11, pp 1440-1461, 2010.

[30] M. Pailha, O. Pouliquen, A two-phase flow description of the initiation of underwater granular avalanches, *J. Fluid Mech.*, Vol. 633, pp 115-135, 2009.

[31] W. Prager, D.C. Drucker, Soil mechanics and plastic analysis or limit design, *Q. Appl. Math.*, Vol. 10(2), pp 157-165, 1952.

[32] P. R. Pokhrel, General Phase-eigenvalues for Two-phase Mass Flows: Supercritical and Subcritical States, MPhil Dissertation, School of Science, Kathmandu University, Nepal, 2014.

[33] P. R. Pokhrel, K. B. Khattri, B. M. Tuladhar, S. P. Pudasaini, A generalized quasi two-phase bulk mixture model for mass flow,*Int. J. of Non-Linear Mech.*, Vol. 99, pp 229-239, 2018.

[34] P. R. Pokhrel, S. P. Pudasaini, Stream function-vorticity formulation of mixture mass flow, *Int. J. of Non-Linear Mech.*, doi: 10.1016/j.ijnonlinmec.2019.103317, 2019.

[35] P. R. Pokhrel, Generalized Quasi Two-Phase Bulk Mixture Models for Mass Flow, PhD Dissertation, School of Science, Kathmandu University, Nepal, 2019.

[36] P. R. Pokhrel, B. M. Tuladhar, Determination of Phase-Eigenvalues by Rational Factorization and Enhanced Simulation of Two-Phase Mass Flow, *Journal of Nepal Mathematical Society*, Vol. 2(2), pp 61-77, 2019.

[37] S. P. Pudasaini, Y. Wang, K. Hutter, Modelling debris flows down general channels, *Nat. Hazards Earth Syst. Sci.*, Vol. 5, pp 799-819, 2005.

[38] S. P. Pudasaini, A general two-phase debris flow model, *Journal of Geophysical Research* Vol. 117(F03010), doi:10.1029/2011JF002186, 2012.

[39] S. P. Pudasaini, Dynamics of submarine debris flow and tsunami, *Acta Mechanica*, Vol. 225(8), pp 2423-2434, 2014.

[40] S. P. Pudasaini, P. Kattel, J. Kafle, Debris flow structure interactions on mountain slopes and reservoirs. In 5th ISHR Europe Congress new challenges in hydraulic research and engineering, Trento, 12-14 June, (Extended Abstract), 2018.

[41] A. von Boetticher, J. M. Turowski, B. W. McArdell, D. Rickenmann, J. W. Kirchner, DebrisInterMixing-2.3: a finite volume solver for three-dimensional debris-flow simulations with two calibration parameters - Part 1: Model description. *Geosci. Model Dev.*, Vol. 9, pp 2909-2923, 2016.

[42] A. von Boetticher, J. M.Turowski, B. W. McArdell, D. Rickenmann, M. Hürlimann, C. Scheidl, J. W. Kirchner, DebrisInterMixing-2.3: a finite volume solver for three-dimensional debris - flow simulations with two calibration parameters - Part 2: Model validation. *Geosci. Model Dev. Discuss.*, Vol. 10(11), 3963-3978, 2017.